

Update of genetic variants in CEP120 and CC2D2A – with an emphasis on genotype-phenotype correlations, tissue specific transcripts and exploring mutation specific exon skipping therapies

Miguel Barroso-Gil¹, Eric Olinger¹, Simon Ramsbottom¹, Elisa Molinari¹, Colin Miles¹, and John Sayer¹

¹Newcastle University

August 25, 2020

Abstract

Mutations in ciliary genes cause a spectrum of both overlapping and distinct clinical syndromes (ciliopathies). CEP120 and CC2D2A are paradigmatic examples for this genetic heterogeneity and pleiotropy as mutations in both cause Joubert syndrome but are also associated with skeletal ciliopathies and Meckel syndrome, respectively. The molecular basis for this phenotypical variability is not understood but basal exon skipping likely contributes to tolerance for deleterious mutations via preservation of the amount of expressed functional protein. Here we systematically review and annotate genetic variants described in CEP120- and CC2D2A-associated disease and confirm more severe clinical presentations with biallelic truncating CC2D2A mutations. Combining in silico and ex vivo studies, we identify alternative basal exon skipping in the kidney, with possible relevance for organ-specific disease manifestations. Finally, we propose a multimodal approach to classify exons amenable to exon skipping and by mapping reported variants, 14 truncating mutations in 7 CC2D2A exons were identified as potentially rescuable by targeted exon skipping, an approach that is already in clinical use for other inherited human diseases. We conclude that genotype-phenotype correlations for CC2D2A support the deleteriousness of null alleles and that CC2D2A, but not CEP120, offers potential for therapeutic exon skipping approaches.

KEYWORDS

Antisense oligonucleotide, CC2D2A, CEP120, ciliopathy, exon skipping, Joubert syndrome, Meckel syndrome, precision medicine

INTRODUCTION

Human disorders arising from the dysfunction of motile and/or primary cilia are collectively referred to as ciliopathies and there are more than a dozen distinguishable ciliopathy syndromes. Within the spectrum of disease arising from defects in the primary cilium (primary ciliopathies) these include, but are not limited to, neurological diseases (e.g. Joubert syndrome (JBTS, MIM PS213300) and Meckel syndrome (MKS, MIM PS249000)), skeletal ciliopathies (e.g. Jeune asphyxiating thoracic dystrophy (JATD), MIM PS208500), kidney diseases (e.g. nephronophthisis (NPHP), MIM PS256100, autosomal dominant and recessive polycystic kidney disease (ADPKD & ARPKD), MIM PS173900) and retinal dystrophies such as Leber congenital amaurosis (LCA, MIM PS120970) (Novarino, Akizu, & Gleeson, 2011; Reiter & Leroux, 2017; Shaheen et al., 2016). Collectively, ciliopathies affect approximately 1 in every 2000 individuals with ADPKD being by far the most common (Kagan, Dufke, & Gembruch, 2017). As well as the high level of phenotypic complexity and overlap of clinical phenotypes, mutations within the same gene can give rise to distinct ciliopathy syndromes, known as genetic pleiotropy (Coppieters, Lefever, Leroy, & De Baere, 2010; Roosing et al., 2016; Shaheen et al., 2016; Shamseldin et al., 2020). In addition, mutations in different genes can cause the same

ciliopathy syndrome (genetic heterogeneity) such as it is the case of JBTS, with more than 35 genes associated (*Figure S1*) (Braun & Hildebrandt, 2017; Mitchison & Valente, 2017; Parisi, 2019). In addition, we have recently shown that differences in phenotypic presentation in patients with the same mutations, is in part due to the presence of genetic modifiers (Ramsbottom et al., 2020). JBTS represents the least severe end in the spectrum of neuronal ciliopathies (Parisi, 2019; Radha Rama Devi, Naushad, & Lingappa, 2020). The cerebellar and brainstem malformation, described as the “molar tooth sign” (MTS), is the hallmark for the diagnosis (Romani, Micalizzi, & Valente, 2013). On the other extreme of the spectrum is MKS, a lethal multiorgan ciliopathy, characterised by central nervous system (CNS) malformations (frequently occipital encephalocele), cystic renal dysplasia, and hepatic abnormalities including ductal plate malformation and hepatic fibrosis (Alexiev, Lin, Sun, & Brenner, 2006; Hartill, Szymanska, Sharif, Wheway, & Johnson, 2017). As an example for genetic pleiotropy and heterogeneity, genetic variants in both *CEP120* and *CC2D2A* have been reported to cause JBTS, with *CEP120* having a tropism for skeletal ciliopathies and *CC2D2A* giving rise to the whole spectrum of neuronal ciliopathies (Bachmann-Gagescu et al., 2012; Mougou-Zerelli et al., 2009; Roosing et al., 2016; Shaheen et al., 2015).

Centrosomal protein of 120 kDa (encoded by *CEP120*) is expressed ubiquitously in embryonic mice tissues with a subcellular expression enriched in the daughter centriole (Mahjoub, Xie, & Stearns, 2010; Xie et al., 2007). Several studies have investigated the role of CEP120 in centriole biogenesis and ciliogenesis and revealed its requirement for centriole duplication, assembly, elongation and maturation (*Table S1 & Table S2*) (Comartin et al., 2013; Mahjoub et al., 2010). Originally, biallelic genetic variants in *CEP120* have been detected in 4 families with JATD but the gene has been linked to JBTS as well in later reports (Roosing et al., 2016; Shaheen et al., 2015). Coiled-coil and C2 domain containing 2A (encoded by *CC2D2A*) is a centrosome-cilia protein that is described to be expressed in multiple human adult tissues, particularly in brain, prostate, pancreas, kidney, lung, liver and retina (Noor et al., 2008). CC2D2A localises and functions at the basal body/mother centriole, in particular, at the transition zone (TZ) (Gorden et al., 2008; Veleri et al., 2014) where it has a role in ciliogenesis (Lewis et al., 2019; Tallila, Jakkula, Peltonen, Salonen, & Kestila, 2008; Veleri et al., 2014) and vesicle trafficking through the TZ (*Table S1 & Table S2*) (Bachmann-Gagescu et al., 2015; Ojeda Naharros et al., 2017; Williams et al., 2011). Mutations in *CC2D2A* cause a spectrum of clinical phenotypes, ranging from isolated rod-cone dystrophy (Mejcase et al., 2019) to JBTS (Bachmann-Gagescu et al., 2012; Gorden et al., 2008; Noor et al., 2008) and MKS (Mougou-Zerelli et al., 2009; Szymanska et al., 2012; Tallila et al., 2008; Tallila, Salonen, Kohlschmidt, Peltonen, & Kestila, 2009). How mutations in these two genes, encoding proteins with different ciliary localization and function, can lead to this wide spectrum of distinct clinical presentations with partially overlapping phenotypes is not fully understood.

In 2015, Drivas *et al.* suggested that basal levels of alternative splicing (AS) with exon skipping may be responsible for some of the genetic pleiotropy observed in *CEP290*- and *CC2D2A*-associated disease (Drivas, Wojno, Tucker, Stone, & Bennett, 2015). AS is a mechanism by which a precursor messenger RNA (pre-mRNA) is processed into multiple isoforms (Nilsen & Graveley, 2010; Tabrez, Sharma, Jain, Siddiqui, & Mukhopadhyay, 2017) and is thought to occur in around 95% of multiexon genes (Pan, Shai, Lee, Frey, & Blencowe, 2008). Basal levels of noncanonical splicing has indeed been shown to occur in patient dermal fibroblasts with *CEP290* mutations but also in control samples. The authors show that deleterious mutations in *CEP290* and *CC2D2A* falling into exons that are in-frame are associated with a higher level of residual near-full length protein, as they escape nonsense-mediated mRNA decay (NMD), and correspond with a milder clinical phenotype (Drivas et al., 2015). Nonsense-associated altered splicing (NAS), an endogenous mechanism increasing the level of alternatively spliced transcripts in response to truncating variants might contribute to this rescue, although no evidence for a selective mechanism was found in this study (Drivas et al., 2015). It is currently unclear whether tissue-specific splicing events could underlie differential organ involvement in ciliopathies.

The potential of therapies exploiting this natural mechanism and based on the specific removal of dispensable exons by exon-skipping antisense oligonucleotides (ASOs) has now been well established (Aartsma-Rus & van Ommen, 2007; Bennett & Swayze, 2010). The treatment of patients with Duchenne muscular dystrophy

(DMD) by targeting specific exons within the disease-causing gene, *DMD*, leads to exon skipping and a subsequent restoration of reading frame and a partially functional dystrophin protein (Aartsma-Rus & van Ommen, 2007; Kole & Krieg, 2015; Komaki et al., 2018; Lee, Saito, Duddy, Takeda, & Yokota, 2018; Servais et al., 2015). The same strategy has recently been applied to nonsense mutations within *CEP290* (Barney et al., 2019; Garanto et al., 2016; Molinari et al., 2019; Ramsbottom et al., 2018) building on the fundamental finding that exon skipping in *CEP290* is tolerated and leads to functional transcripts (Drivas et al., 2015). ASO-mediated exon skipping rescued the ciliary phenotype and CEP290 protein levels in a humanised murine model of Leber congenital amaurosis (LCA) (Garanto et al., 2016) and intravitreal injections of ASOs improved visual acuity in LCA patients (Cideciyan et al., 2019). Systemic administration of ASOs via intravenous injections was shown to induce skipping of a gene trap in a JBTS mouse model restoring CEP290 protein levels and rescuing renal ciliary phenotype and the cystic burden in the kidneys (Ramsbottom et al., 2018). As a proof of principle, *ex-vivo* ASO-mediated skipping restored the ciliary phenotype in human urine-derived renal epithelial cells (hURECs) and fibroblasts derived from a JBTS patient carrying a *CEP290* homozygous truncating mutation (Molinari et al., 2019; Ramsbottom et al., 2018).

In this study, we systematically review and curate genetic variants and phenotypes associated with *CEP120* and *CC2D2A*, two genes paradigmatic for the concepts of genetic heterogeneity and pleiotropy, and investigate genotype-phenotype correlations. Extending the concept proposed by Drivas et al. (Drivas et al., 2015; Molinari, Srivastava, Sayer, & Ramsbottom, 2017; Rozet & Gerard, 2015), we detect and validate tissue-specific splicing events and, using these two genes, propose a multimodal approach to identify target exons for future exon skipping therapy approaches.

RESULTS

Genetic and clinical spectra of ciliopathies caused by biallelic variants in *CEP120* and *CC2D2A*

We screened PubMed® for reports of patients harbouring biallelic genetic variants in *CEP120* or *CC2D2A*, accessed the Human Gene Mutation Database (HGMD®) for additional entries and manually curated the genetic and phenotypic data available in order to create a comprehensive database for *CEP120* - and *CC2D2A* -associated disease compliant with Human Genome Variation Society (HGVS) recommendations.

To date, only nine index patients harbouring homozygous or compound heterozygous genetic variants in *CEP120* have been reported. 4/9 presented with JBTS, 3/9 with Jeune asphyxiating thoracic dystrophy (JATD), 1/9 with a MKS/oro-facial-digital syndrome (OFD) overlap and 1/9 with tectocerebellar dysraphia with occipital encephalocele (TCDOE) (Table 1 & Figure S2A). In these patients, 14 missense alleles, 3 frameshift alleles and 1 nonsense allele are reported, in different combinations (Table 1 & Table S4 & Figure S2B). Variant p.Ala199Pro alone is found in homozygosis in 3 index patients and in compound heterozygote state in another patient (representing 7/14 missense alleles) (Roosing et al., 2016; Shaheen et al., 2015). The *CEP120* variant p.Leu712Phe is reported in compound heterozygote state in one patient (Roosing et al., 2016) (MTI-143, Table 1) but population data indicate an allelic frequency of ~0.004 with 2 homozygous individuals in the normal population (<https://gnomad.broadinstitute.org/>) (Table S4). Although *in vitro* experiments indicated that this variant impairs the recruitment of Talpid3 to the centrioles, its pathogenicity is questionable (Tsai, Hsu, Liu, Chang, & Tang, 2019).

103 patients from 91 families suffering from *CC2D2A* -related disease have been reported to date (Table 2 & Table S3). Roughly half of the patients suffered from JBTS or Joubert syndrome related disorders (JSRD) (32/103 and 18/103 respectively), with slightly less than half displaying an MKS (40/103) or Meckel syndrome-like (ML) presentation (3/103). Rare cases were described with rod-cone dystrophy (RCD) (4/103), Cogan-type congenital oculomotor apraxia (1/103) or autism-spectrum disease (1/103). In 4 reported cases, the phenotype was not unequivocally described (Figure 1A & Table S3). When considering only the index patients, 83 missense alleles were detected, followed by frameshift (n=60), splice-affecting (n=19) and nonsense (n=16) alleles and rare single AA deletions (n=2) or large insertions/deletions (n=4), including one reported case of retrotransposon insertion (Figure 1B & Table S3). Altogether, 75 different ge-

netic variants have been identified in the 91 reported families (Table S5). *CC2D2A* variants p.Glu229del and p.Pro721Ser have been each detected in 1 patient in compound heterozygosis or homozygosis, respectively (Table S3) (Mougou-Zerelli et al., 2009; Otto et al., 2011). The allelic frequency in gnomAD is 0.062 for the former (incl. 528 homozygous individuals) and 0.002 for the latter (incl. 3 homozygous carriers) (Table S5), suggesting that these are hypomorphic alleles rather than fully pathogenic variants (Bachmann-Gagescu et al., 2012).

Genotype-phenotype correlations in disease caused by mutations in *CC2D2A*

Having now systematically assessed the variants in *CC2D2A* and the associated phenotypes for all 103 reported patients, we wondered whether truncating variants (nonsense or frameshift) were associated with a more severe phenotype than missense variants, as suggested before (Mougou-Zerelli et al., 2009). Biallelic truncating variants were found in 66% (21/32) of cases presenting with MKS or ML, contrasting with only 3% (1/40) of cases presenting with JBTS or JSRD (Fisher’s exact test: $p < 0.0001$). Conversely, biallelic missense variants were detected in only 22% (7/32) of MKS/ML cases vs. 53% (21/40) of cases with JBTS/JSRD (Fisher’s exact test: $p = 0.0143$) (Figure 1C & Figure 1D). This systematic analysis of all reported cases to date shows a robust correlation between the type of *CC2D2A* mutation and the severity of the disease. What is more, we assessed systematically the cases reported in literature with specific mention of either presence or absence of kidney disease and we show that biallelic truncating variants were more frequently found in presence of kidney disease (50%, 20/40) than in cases without kidney involvement (3%, 1/32) (Fisher’s exact test: $p < 0.0001$), in line with the notion that missense changes are more frequently associated with a pure JBTS presentation without extra-CNS manifestations (Figure 1E & Figure 1F). Similar associations were not seen for *CEP120* but a meaningful analysis was precluded by the low patient numbers (Figure S2C & Figure S2D).

In silico analysis of gene expression and tissue-specific basal exon skipping

Based on these results suggesting that truncating variants are associated with a more severe clinical picture, we were interested to assess the applicability of exon skipping therapies to rescue truncating variants (Ramsbottom et al., 2018). Basal exon skipping events are particularly informative as they indicate that skipping of these particular exons is likely well tolerated.

CEP120 and *CC2D2A* are ubiquitously expressed in human tissues, with highest expression levels in the female reproductive system and cerebellum for the former and smooth muscle and female reproductive system for the latter (Figure S3). Expression of both genes has also been reported in the human kidney (Figure S3 & <http://www.proteinatlas.org>, (Uhlén et al., 2015)). Cerebellum and kidney phenotypes are classically encountered in ciliopathies (Bachmann-Gagescu et al., 2012; Vilboux et al., 2017). Using human RNA sequencing data available through the Genotype-Tissue Expression (GTEx) project (<https://www.gtexportal.org/home/>), we investigated the tissue-specific expression and splicing of *CEP120* and *CC2D2A* in kidney and cerebellum. ENST00000306481 (“transcript 1”) is the main *CEP120* transcript detected in the kidney medulla and the cerebellar hemisphere. Abundant expression of ENST00000328236 (“transcript 2”) and ENST00000306467 (“transcript 3”) were also detected in the cerebellum but nearly absent in the kidney (Figure 2Ai). These transcript isoforms are generated through alternative splicing events at the pre-mRNA 5’-end, with exon 2 (ref.: ENST00000328236 or NM_153223) predicted to be skipped in the kidney (Figure 2Aii). These changes are reflected by a predicted protein product lacking the first 26 amino acids for transcript 1 (Figure 2Aiii).

For *CC2D2A*, the main protein coding transcripts in kidney medulla are ENST00000515124 (“transcript 1”) and ENST00000503292 (“transcript 2”) and in the cerebellar hemisphere are “transcript 2” and ENST00000389652 (“transcript 3”) (Figure 2Bi). Transcript 1 is short (1474bp), lacking functional CC2D2A domains and generated by splicing in an additional exon after exon 5 (ref.: ENST00000503292), leading to a premature stop codon. This transcript is supported by the detection in GTEx of the specific junction in nearly all tissues but enriched in the kidney (Figure 2Bii). Transcript 3 is detected in cerebellum but not kidney and has an incomplete open reading frame with the 5’-end not fully annotated. However, based on GTEx junction expression data, exon 2 appears to be spliced in the kidney but not the cerebellum, while an

exon predicted in the cerebellum (between exons 30 and 31) is skipped in the kidney. Of interest, a splice junction leading to skipping of exon 30 is detected at low frequency and almost exclusively in the kidney medulla (Figure 2Bii). On the protein level, transcript 1 encodes a 111 amino acid product, sharing the first 82 amino acids with canonical transcript 2 (Figure 2Biii). In summary, human RNAseq data suggest the presence of tissue-specific transcripts for *CEP120* and *CC2D2A*. Exons that are predicted to undergo organ-specific splicing events, such as exon 30 of *CC2D2A*, represent optimal candidates to apply exon skipping strategies. Isoform expression predicted from RNA sequencing data must however be interpreted with caution and specific isoforms should be confirmed by dedicated RT-PCR (Molinari et al., 2018).

Confirmation of tissue-specific basal exon skipping and possible implications for organ disease manifestations

We performed RT-PCR on total RNA from whole blood, kidney and human urine-derived renal epithelial cells (hURECs) using a primer pair targeted to exon 29 and exon 31 from the canonical *CC2D2A* transcript (ENST00000503292). Beside the predicted amplification product of 327bp detected in the kidney and whole blood (at lower levels), a shorter transcript is clearly seen in the kidney but not in whole blood RNA. The observed molecular weight (~150bp), in line with the expected size of an amplification product lacking exon 30 (150bp), strongly suggests basal exon 30 skipping in the kidney (Figure 3A). Furthermore, we were able to detect this basal exon skipping event in hURECs (Figure 3A, right panel), highlighting the utility of this system to study kidney-specific splicing events (Molinari et al., 2018). Given that truncating *CC2D2A* variants are associated with more severe disease and a generally high penetrance for kidney disease (Figure 1) as well as our observation that *CC2D2A* exon 30 undergoes basal exon skipping in the kidney, we wondered whether truncating variants in exon 30 are rescued and therefore tolerated in the kidney. To assess this hypothesis, we represented the relative prevalence of kidney disease associated with truncating variants in the different *CC2D2A* exons (Figure 3B). Unfortunately, only 2 patients harboured a truncating variant in exon 30 limiting the strength of our conclusions. However, neither of these patients showed kidney involvement as compared with kidney disease in 33.3-100% of truncating variants in the other exons (Figure 3B). Considering all patients with either monoallelic or biallelic truncating variants, 35/48 presented with kidney disease vs only 13 that did not present kidney disease (including the 2 patients with exon 30 truncating variants). Patient MTI-991 (Table 1) harboured a *CEP120* biallelic intronic variant at the exon-intron boundary 3' of exon 2 and shown to lead to intron retention (Roosing et al., 2016). However, as exon 2 appears to be skipped in the kidney (Figure 2), this variant is likely "silent" in the kidney. Indeed, this patient did not show kidney involvement (Roosing et al., 2016).

Multimodal identification of skippable exons in *CEP120* and *CC2D2A* and mapping of reported truncating mutations

The *CEP120* transcript ENST00000328236 contains 20 coding exons. Among them, the nucleotide length of 11 exons is a multiple of three and therefore amenable to exon skipping without change in reading frame (Figure 4A). Considering the location of protein domains of functional importance (coiled-coil and C2 domains), only exons 14 and 15 are predicted to be skippable without inducing loss of protein function. As codons are not overlapping between exons (phase 0), skipping of exons 14 and 15 will not lead to potential amino acid substitutions. Based on the GTEx alternative splicing data presented above, exon 2 (predicted to be skipped in kidney, see transcript ENST00000306481) might represent an additional target for tolerated exon skipping with an alternative start codon functional in exon 3. However, none of the reported *CEP120* mutations to date fall in either one of these identified exons, suggesting that *CEP120*, at the current state of knowledge, is not a good candidate gene to apply exon skipping therapies.

The *CC2D2A* transcript ENST00000503292 contains 36 coding exons, 17 of which are amenable to exon skipping without change in reading frame (Figure 4B). Considering the location of protein domains of functional importance (coiled-coil and C2 domains) (Bachmann-Gagescu et al., 2012; Noor et al., 2008) exons 4, 7, 8, 9, 12, 13, 22, 23, 31, 32, 33, 34 and 35 might be skippable without inducing loss of protein function. These exons all contain full complements of codons (phase 0) and can therefore be skipped without introducing potential amino acid substitutions. Based on the data presented above, exon 30 appears as another promising

candidate for exon skipping. Furthermore, exon 30 is predicted to encode only the last 3 amino acids of the C2 domain or to have no overlap with the C2 domain at all (Bachmann-Gagescu et al., 2012; Gorden et al., 2008; Noor et al., 2008; Srour et al., 2012). Prediction tools and available literature provide conflicting data with respect to C2 domain overlap with exon 25, indicating the need for functional studies confirming this potential exon skipping target (<http://smart.embl-heidelberg.de/>) (Bachmann-Gagescu et al., 2012; Noor et al., 2008; Srour et al., 2012). Because of their clear pathogenic implications, we focus on truncating variants as potential targets for exon skipping approaches. Table 2 lists the reported patients harbouring at least one truncating variants, in any of the *CC2D2A* skippable exons. Furthermore, all *CC2D2A* truncating variants falling into any of the predicted skippable exons are represented in Figure 4B. 14 different truncating variants represent potential targets for exon skipping and are located in exons 8, 13, 22, 23, 25, 30 and 31 (Figure 4B). Four of these truncating variants have been described in homozygosis: c.517C>T (p.Arg173Ter, exon 8), c.2848C>T (p.Arg950Ter, exon 23), c.2875del (p. Glu959AsnfsTer3, exon 23) and c.3084del (p. Lys1029ArgfsTer3, exon 25). Skipping of each of the 7 identified exons that harbour truncating variants and are potentially tolerant to skipping is leading to a predicted near-full length protein product (Figure S4).

DISCUSSION

CEP120 and *CC2D2A* both encode ciliary proteins, with a different subcellular localization and function. Mutations in these genes are associated with a spectrum of both overlapping and distinct ciliopathies illustrating the concepts of genetic heterogeneity and pleiotropy, inherent to most ciliopathy genes. To capture the genetic and clinical spectrum of *CEP120* - and *CC2D2A* -associated disease, we reviewed literature, including previous mutation summaries (Bachmann-Gagescu et al., 2012; Lam, Albaba, Study, & Balasubramanian, 2020), and open-access tools to generate a curated, annotated and HGVS compliant database. Furthermore, we used *in silico* tools to identify tissue-specific basal exon skipping events. Using this database, we establish genotype-phenotype correlations, including possible insights into tissue-specific disease expression, and show that several exons in *CC2D2A*, but not in *CEP120*, are good candidates for future exon skipping approaches. In addition to creating an updated and annotated database for *CEP120* - and *CC2D2A* - associated disease, we provide a possible roadmap of how open-access tools can be used to identify future targets for splice-altering therapeutic approaches.

To date, only 9 patients from 9 different families have been described with biallelic genetic variants in *CEP120* and 103 patients from 91 families with biallelic variants in *CC2D2A*. In these patient populations, 9 different genetic variants have been described in *CEP120* and 75 different variants in *CC2D2A*. It has been previously shown that mutations in *CC2D2A* cluster to the C-terminal half of the protein (Bachmann-Gagescu et al., 2012) (Figure 4B). Several variants are shared between unrelated families and might follow geographical clusters. For instance, *CC2D2A* variant c.1762C>T was detected in 11 unrelated cases with MKS in the Finnish population but not reported outside Scandinavia (Tallila et al., 2008). In contrast, *CC2D2A* missense variant c.4667A>T is found in 13 unrelated cases, always in compound heterozygous state and without apparent geographical patterns. Finally, by crossing purported disease-causing variants with genomic data from the general population, we detected common variants (*CC2D2A*: p.Glu229del & p.Pro721Ser; *CEP120*: p.Leu712Phe) that are most likely misclassified, echoing similar concerns for other ciliopathy genes (Pauli et al., 2019; Shaheen et al., 2016).

Mutations in *CC2D2A* is a common cause of ciliopathy accounting for 7.7% of JBTS and 10% of MKS in a previous large cohort study (Bachmann-Gagescu et al., 2012). The relative prevalence of this disease enabled more detailed analyses of genotype-phenotype correlations that are important to prioritize genetic testing (if targeted tests are performed), provide better prognostic information but can also give insights into disease mechanisms. Previous studies showed that subjects with *CC2D2A*-related JBTS were more likely to have ventriculomegaly and seizures than subjects without *CC2D2A* mutations (Bachmann-Gagescu et al., 2012). Furthermore, it has been previously noted that patients with at least one missense mutation in *CC2D2A* are more likely to suffer from JBTS while patients with biallelic truncating variants display more often MKS or ML, in line with a more deleterious effect of null alleles (Bachmann-Gagescu et al., 2012; Mougou-Zerelli et al., 2009). A similar correlation between biallelic truncating variants and more severe phenotypes has been

suggested for the ciliopathy genes *TMEM67* and *RPGRIP1L* (Delous et al., 2007; Iannicelli et al., 2010). In this study, we provide a systematic analysis of all reported patients with *CC2D2A* mutations and indeed show a strikingly more severe clinical presentation for carriers of biallelic null variants. Out of 40 patients with *CC2D2A*-related JBTS/JSRD, only 1 harboured biallelic truncating variants, whereas the majority of *CC2D2A*-related MKS/ML was caused by biallelic null alleles. We also show that this association holds true for extra-CNS manifestations as patients with biallelic truncating variants were strikingly more likely to suffer from kidney disease (Figure 1). This observation is compatible with the notion that some of the observed genetic pleiotropy might be explained by the effects of particular mutations on total protein expression. In support of this hypothesis, Drivas et al. showed that basal exon skipping events modulate total protein expression in patients with *CEP290* and *CC2D2A* mutations and that protein expression inversely correlated with disease severity (Drivas et al., 2015). Large-scale human sequencing projects suggest major differences in pre-mRNA splicing and basal exon skipping between different organs for most of our transcriptome. Whether these tissue-specificities contribute to genetic pleiotropy is currently unknown. Here, we provide *ex vivo* data showing tissue-specific differences in basal exon skipping and illustrate how these effects might be exploited for a better understanding of different organ involvement in ciliopathies. While our limited data by no means prove this concept, we estimate that this is an exciting field for future studies. As alternative splicing events are conserved in human urine-derived epithelial cells (hURECs), they provide the ideal tool to investigate splicing in the kidney (Figure 3) (Molinari et al., 2018).

Using bioinformatic tools, including sequence data, domain annotations and alternative splicing predictions, we identified potentially skippable exons in *CC2D2A* and *CEP120* and populated them with reported truncating variants to assess the applicability of therapeutic exon skipping for these two ciliopathy genes. Only exons 14 and 15 in *CEP120* are skippable without inducing a frameshift or disrupting a functional domain. None of the reported genetic variants to date map into these two exons. Given the low number of mutations reported, it is currently impossible to say whether this is purely down to chance or whether this observation reflects the fact that these particular exons are functionally not important and/or skippable and therefore mutations in these exons are tolerated. In contrast, we identify 15/38 exons in *CC2D2A* as potentially skippable and we mapped 14 distinct truncating variants in 7 of them. Exon 30 appears to be a particularly good candidate as this exon undergoes basal exon skipping in the kidney, potentially modulating the severity of kidney disease associated with JBTS-causing truncating mutations therein. This example highlights how open-access databases for tissue-specific splicing could be used to refine targets for exon skipping therapy and suggests exon 30 skipping as a potential therapeutic option for future patients with kidney, liver or retinal involvement arising from truncating mutations in exon 30. Indeed, the *CC2D2A* mutations identified in a total of 26 patients are a starting point for *in vitro* analysis to determine if a functional rescue using antisense oligonucleotide mediated exon skipping is possible. Our group has previously applied ASO-mediated exon skipping to rescue kidney phenotypes in a mouse ciliopathy model (Ramsbottom et al., 2018). Delivery of ASO via systemic administration to the kidney appears effective in contrast to the brain and retinal tissues where blood-brain and blood-retinal barriers respectively cause reduction in delivery (Daneman & Prat, 2015; Himawan et al., 2019; Pardridge, 2002; Yu et al., 2007). In rodents, systemic administration of ASOs revealed greatest accumulation in kidney and liver (Geary, Norris, Yu, & Bennett, 2015; Zhao et al., 1998) and abundant proximal tubular uptake (Janssen et al., 2019; Oberbauer, Schreiner, & Meyer, 1995). Given the high morbidity associated with kidney disease, the potential for adequate ASO delivery, the tissue-specific splicing events that convey important information about potential target exons and the availability of relevant cell systems (hURECs) for non-invasive validation, ASO-mediated exon skipping offers exciting therapeutic perspectives for nephrology and particularly ciliopathy patients suffering from kidney disease (Molinari et al., 2018; Molinari et al., 2019). As this approach was successfully tested in pre-clinical models (Ramsbottom et al., 2018), the next big step is to bring this innovative therapy from bench to bedside, following the path set out by other diseases including Duchenne muscular dystrophy (Kole & Krieg, 2015; Komaki et al., 2018; Lee et al., 2018; Servais et al., 2015).

MATERIAL & METHODS

Web Resources

The URLs for data presented herein are as follows:

Ensembl (release 100): <https://www.ensembl.org/index.html>

Ensembl VEP: <https://www.ensembl.org/info/docs/tools/vep/index.html>

GnomAD v2.1.1: <https://gnomad.broadinstitute.org/>

GTEX: <https://www.gtexportal.org/home/>

The Genotype-Tissue Expression (GTEx) Project was supported by the Common Fund of the Office of the Director of the National Institutes of Health, and by NCI, NHGRI, NHLBI, NIDA, NIMH, and NINDS. The data used for the analyses described in this manuscript were obtained from: the GTEx Portal on 15/02/2020.

HGMD®: <http://www.hgmd.cf.ac.uk/ac/index.php>

NCBI ClinVar: <https://www.ncbi.nlm.nih.gov/clinvar/>

NCBI Primer-BLAST: <https://www.ncbi.nlm.nih.gov/tools/primer-blast/index.cgi>

ProteinPaint: <https://pecan.stjude.cloud/proteinpaint> (Zhou et al., 2016)

PubMed: <https://pubmed.ncbi.nlm.nih.gov/>

SMART: <http://smart.embl-heidelberg.de/>

Varsome®: <https://varsome.com/>

Online Mendelian Inheritance in Man, OMIM®. McKusick-Nathans Institute of Genetic Medicine, Johns Hopkins University (Baltimore, MD), (Hamosh, Scott, Amberger, Valle, & McKusick, 2000). World Wide Web URL: <https://omim.org/>

Patient database

We searched PubMed® and HGMD® (Stenson et al., 2017) databanks (last query 05/2020) for reported patients with biallelic genetic variants in *CEP120* and *CC2D2A* and detected 31 relevant publications. All genetic variants were manually curated and annotated using Ensembl Variant Effect Predictor (Ensembl release 100) (Yates et al., 2020), NCBI ClinVar and VarSome (Kopanos et al., 2019), matched with allele frequency data from the general population assessed via gnomAD v2.1.1. (Karczewski et al., 2020) and compiled using an identifier following the HGVS identification standard (den Dunnen et al., 2016). Patients reported in multiple publications were only included once in our database (if possible to detect) and patients with incomplete genetic or phenotypic information were not included. For each included patient, available phenotypic data were reviewed and where necessary adapted with following disease categories (Drivas et al., 2015): JBTS: All patients with hypoplasia of the cerebellar vermis and/or brain stem abnormalities and often intellectual disability; JSRD: JBTS with extra-CNS manifestations; Meckel-like syndrome (ML): lethality during the first months or years, characterized by cystic kidney disease, CNS malformation (typically DandyWalker malformation), polydactyly, and hepatic fibrosis; MKS: Similar to ML but uniformly perinatal lethal with occipital encephalocele being the predominant CNS malformation.

RNA preparation and RT-PCR

Total RNA from human kidney (ThermoFisher AM7976) was used together with total RNA from whole blood samples and urine-derived renal epithelial cells (hUREC) isolated using RNeasy mini kit (Qiagen) according to the manufacturer's instructions and quantified using a NanoDrop 2000 spectrophotometer. 0.75µg RNA was reverse-transcribed using an oligo-dT primer and SuperScript III Reverse Transcriptase (Thermo Fisher Scientific). The resulting cDNA was used for PCR with a GoTaq® DNA Polymerase (Promega) and a *CC2D2A* gene- specific primer pairs (5- TGAGAGACACTGGCTGGGAT -3 and 5- AG-GCACTGACGATTGGAAAC -3) to identify basal skipping of exon 30. Primers were designed using NCBI Primer-BLAST (<https://www.ncbi.nlm.nih.gov/tools/primer-blast/index.cgi>). Amplification of *HPRT1*

housekeeping gene cDNA was performed alongside. Product electrophoresis was performed on a 2% agarose gel.

ACKNOWLEDGEMENTS

Miguel Barroso-Gil is funded by Kidney Research UK (ST_001_20171120) and the Northern Counties Kidney Research Fund.

Eric Olinger is supported by an Early Postdoc Mobility Stipendium of the Swiss National Science Foundation (P2ZHP3_195181) and Kidney Research UK (Paed_RP_001_20180925).

Elisa Molinari is Funded by Kidney Research UK (RP_006_20180227).

John Sayer and Colin Miles are funded by Kidney Research UK and the Northern Counties Kidney Research Fund.

DATA AVAILABILITY STATEMENT

The data that support the findings of this study are available through The Human Gene Mutation Database at <http://www.hgmd.cf.ac.uk/ac/index.php> and PubMed® at <https://pubmed.ncbi.nlm.nih.gov>. Data presented here were derived from the following resources available in the public domain: The Genotype-Tissue Expression (GTEx) Project (<https://www.gtexportal.org/home/>), The Genome Aggregation Database v2.1.1 (<https://gnomad.broadinstitute.org/>) and Ensembl (release 100): (<https://www.ensembl.org/index.html>).

CONFLICT OF INTEREST

The authors declare no conflict of interest.

REFERENCES

- Aartsma-Rus, A., & van Ommen, G. J. (2007). Antisense-mediated exon skipping: a versatile tool with therapeutic and research applications. *Rna*, 13 (10), 1609-1624. doi:10.1261/rna.653607
- Al-Hamed, M. H., Kurdi, W., Alsahan, N., Alabdullah, Z., Abudraz, R., Tulbah, M., . . . Albaqumi, M. (2016). Genetic spectrum of Saudi Arabian patients with antenatal cystic kidney disease and ciliopathy phenotypes using a targeted renal gene panel. *J Med Genet*, 53 (5), 338-347. doi:10.1136/jmedgenet-2015-103469
- Alexiev, B. A., Lin, X., Sun, C. C., & Brenner, D. S. (2006). Meckel-Gruber syndrome: pathologic manifestations, minimal diagnostic criteria, and differential diagnosis. *Arch Pathol Lab Med*, 130 (8), 1236-1238. doi:10.1043/1543-2165(2006)130[1236:Ms]2.0.Co;2
- Bachmann-Gagescu, R., Dona, M., Hettterschijt, L., Tonnaer, E., Peters, T., de Vrieze, E., . . . van Wijk, E. (2015). The Ciliopathy Protein CC2D2A Associates with NINL and Functions in RAB8-MICAL3-Regulated Vesicle Trafficking. *PLoS Genet*, 11 (10), e1005575. doi:10.1371/journal.pgen.1005575
- Bachmann-Gagescu, R., Ishak, G. E., Dempsey, J. C., Adkins, J., O'Day, D., Phelps, I. G., . . . Doherty, D. (2012). Genotype-phenotype correlation in CC2D2A-related Joubert syndrome reveals an association with ventriculomegaly and seizures. *J Med Genet*, 49 (2), 126-137. doi:10.1136/jmedgenet-2011-100552
- Barny, I., Perrault, I., Michel, C., Goudin, N., Defoort-Dhellemmes, S., Ghazi, I., . . . Gerard, X. (2019). AON-Mediated Exon Skipping to Bypass Protein Truncation in Retinal Dystrophies Due to the Recurrent CEP290 c.4723A > T Mutation. Fact or Fiction? *Genes (Basel)*, 10 (5). doi:10.3390/genes10050368
- Ben-Salem, S., Al-Shamsi, A. M., Gleeson, J. G., Ali, B. R., & Al-Gazali, L. (2014). Mutation spectrum of Joubert syndrome and related disorders among Arabs. *Hum Genome Var*, 1 , 14020. doi:10.1038/hgv.2014.20
- Ben-Salem, S., Al-Shamsi, A. M., Gleeson, J. G., Ali, B. R., & Al-Gazali, L. (2015). Erratum: Mutation spectrum of Joubert syndrome and related disorders among Arabs. *Hum Genome Var*, 2 , 15001. doi:10.1038/hgv.2015.1

- Bennett, C. F., & Swayze, E. E. (2010). RNA targeting therapeutics: molecular mechanisms of antisense oligonucleotides as a therapeutic platform. *Annu Rev Pharmacol Toxicol*, 50 , 259-293. doi:10.1146/annurev.pharmtox.010909.105654
- Braun, D. A., & Hildebrandt, F. (2017). Ciliopathies. *Cold Spring Harb Perspect Biol*, 9 (3). doi:10.1101/cshperspect.a028191
- Cideciyan, A. V., Jacobson, S. G., Drack, A. V., Ho, A. C., Charnig, J., Garafalo, A. V., . . . Russell, S. R. (2019). Effect of an intravitreal antisense oligonucleotide on vision in Leber congenital amaurosis due to a photoreceptor cilium defect. *Nat Med*, 25 (2), 225-228. doi:10.1038/s41591-018-0295-0
- Comartin, D., Gupta, G. D., Fussner, E., Coyaude, E., Hasegan, M., Archinti, M., . . . Pelletier, L. (2013). CEP120 and SPICE1 cooperate with CPAP in centriole elongation. *Curr Biol*, 23 (14), 1360-1366. doi:10.1016/j.cub.2013.06.002
- Coppieters, F., Lefever, S., Leroy, B. P., & De Baere, E. (2010). CEP290, a gene with many faces: mutation overview and presentation of CEP290base. *Hum Mutat*, 31 (10), 1097-1108. doi:10.1002/humu.21337
- Daneman, R., & Prat, A. (2015). The blood-brain barrier. *Cold Spring Harb Perspect Biol*, 7 (1), a020412. doi:10.1101/cshperspect.a020412
- Delous, M., Baala, L., Salomon, R., Laclef, C., Vierkotten, J., Tory, K., . . . Saunier, S. (2007). The ciliary gene RPGRIP1L is mutated in cerebello-oculo-renal syndrome (Joubert syndrome type B) and Meckel syndrome. *Nat Genet*, 39 (7), 875-881. doi:10.1038/ng2039
- den Dunnen, J. T., Dalgleish, R., Maglott, D. R., Hart, R. K., Greenblatt, M. S., McGowan-Jordan, J., . . . Taschner, P. E. (2016). HGVS Recommendations for the Description of Sequence Variants: 2016 Update. *Hum Mutat*, 37 (6), 564-569. doi:10.1002/humu.22981
- Doherty, D., Parisi, M. A., Finn, L. S., Gunay-Aygun, M., Al-Mateen, M., Bates, D., . . . Glass, I. A. (2010). Mutations in 3 genes (MKS3, CC2D2A and RPGRIP1L) cause COACH syndrome (Joubert syndrome with congenital hepatic fibrosis). *J Med Genet*, 47 (1), 8-21. doi:10.1136/jmg.2009.067249
- Drivas, T. G., Wojno, A. P., Tucker, B. A., Stone, E. M., & Bennett, J. (2015). Basal exon skipping and genetic pleiotropy: A predictive model of disease pathogenesis. *Sci Transl Med*, 7 (291), 291ra297. doi:10.1126/scitranslmed.aaa5370
- Garanto, A., Chung, D. C., Duijkers, L., Corral-Serrano, J. C., Messchaert, M., Xiao, R., . . . Collin, R. W. (2016). In vitro and in vivo rescue of aberrant splicing in CEP290-associated LCA by antisense oligonucleotide delivery. *Hum Mol Genet*, 25 (12), 2552-2563. doi:10.1093/hmg/ddw118
- Geary, R. S., Norris, D., Yu, R., & Bennett, C. F. (2015). Pharmacokinetics, biodistribution and cell uptake of antisense oligonucleotides. *Adv Drug Deliv Rev*, 87 , 46-51. doi:10.1016/j.addr.2015.01.008
- Gorden, N. T., Arts, H. H., Parisi, M. A., Coene, K. L., Letteboer, S. J., van Beersum, S. E., . . . Doherty, D. (2008). CC2D2A is mutated in Joubert syndrome and interacts with the ciliopathy-associated basal body protein CEP290. *Am J Hum Genet*, 83 (5), 559-571. doi:10.1016/j.ajhg.2008.10.002
- Hamosh, A., Scott, A. F., Amberger, J., Valle, D., & McKusick, V. A. (2000). Online Mendelian Inheritance in Man (OMIM). *Hum Mutat*, 15 (1), 57-61. doi:10.1002/(SICI)1098-1004(200001)15:1<57::AID-HUMU12>3.0.CO;2-G
- Hartill, V., Szymanska, K., Sharif, S. M., Wheway, G., & Johnson, C. A. (2017). Meckel-Gruber Syndrome: An Update on Diagnosis, Clinical Management, and Research Advances. *Front Pediatr*, 5 , 244. doi:10.3389/fped.2017.00244
- Himawan, E., Ekstrom, P., Buzgo, M., Gaillard, P., Stefansson, E., Marigo, V., . . . Paquet-Durand, F. (2019). Drug delivery to retinal photoreceptors. *Drug Discov Today*, 24 (8), 1637-1643. doi:10.1016/j.drudis.2019.03.004

- Hopp, K., Heyer, C. M., Hommerding, C. J., Henke, S. A., Sundsbak, J. L., Patel, S., . . . Harris, P. C. (2011). B9D1 is revealed as a novel Meckel syndrome (MKS) gene by targeted exon-enriched next-generation sequencing and deletion analysis. *Hum Mol Genet*, *20* (13), 2524-2534. doi:10.1093/hmg/ddr151
- Iannicelli, M., Brancati, F., Mougou-Zerelli, S., Mazzotta, A., Thomas, S., Elkhartoufi, N., . . . Valente, E. M. (2010). Novel TMEM67 mutations and genotype-phenotype correlates in meckelin-related ciliopathies. *Hum Mutat*, *31* (5), E1319-1331. doi:10.1002/humu.21239
- Janssen, M. J., Nieskens, T. T. G., Steevens, T. A. M., Caetano-Pinto, P., den Braanker, D., Mulder, M., . . . Wilmer, M. J. (2019). Therapy with 2'-O-Me Phosphorothioate Antisense Oligonucleotides Causes Reversible Proteinuria by Inhibiting Renal Protein Reabsorption. *Mol Ther Nucleic Acids*, *18* , 298-307. doi:10.1016/j.omtn.2019.08.025
- Jones, D., Fiozzo, F., Waters, B., McKnight, D., & Brown, S. (2014). First-trimester diagnosis of Meckel-Gruber syndrome by fetal ultrasound with molecular identification of CC2D2A mutations by next-generation sequencing. *Ultrasound Obstet Gynecol*, *44* (6), 719-721. doi:10.1002/uog.13381
- Kagan, K. O., Dufke, A., & Gembruch, U. (2017). Renal cystic disease and associated ciliopathies. *Curr Opin Obstet Gynecol*, *29* (2), 85-94. doi:10.1097/GCO.0000000000000348
- Karczewski, K. J., Francioli, L. C., Tiao, G., Cummings, B. B., Alfoldi, J., Wang, Q., . . . MacArthur, D. G. (2020). The mutational constraint spectrum quantified from variation in 141,456 humans. *Nature*, *581* (7809), 434-443. doi:10.1038/s41586-020-2308-7
- Kole, R., & Krieg, A. M. (2015). Exon skipping therapy for Duchenne muscular dystrophy. *Adv Drug Deliv Rev*, *87* , 104-107. doi:10.1016/j.addr.2015.05.008
- Komaki, H., Nagata, T., Saito, T., Masuda, S., Takeshita, E., Sasaki, M., . . . Takeda, S. (2018). Systemic administration of the antisense oligonucleotide NS-065/NCNP-01 for skipping of exon 53 in patients with Duchenne muscular dystrophy. *Sci Transl Med*, *10* (437). doi:10.1126/scitranslmed.aan0713
- Kopanos, C., Tsiolkas, V., Kouris, A., Chapple, C. E., Albarca Aguilera, M., Meyer, R., & Massouras, A. (2019). VarSome: the human genomic variant search engine. *Bioinformatics*, *35* (11), 1978-1980. doi:10.1093/bioinformatics/bty897
- Lam, Z., Albaba, S., Study, D., & Balasubramanian, M. (2020). Atypical, milder presentation in a child with CC2D2A and KIDINS220 variants. *Clin Dysmorphol*, *29* (1), 10-16. doi:10.1097/MCD.0000000000000298
- Lee, J. J. A., Saito, T., Duddy, W., Takeda, S., & Yokota, T. (2018). Direct Reprogramming of Human DMD Fibroblasts into Myotubes for In Vitro Evaluation of Antisense-Mediated Exon Skipping and Exons 45-55 Skipping Accompanied by Rescue of Dystrophin Expression. *Methods Mol Biol*, *1828* , 141-150. doi:10.1007/978-1-4939-8651-4_8
- Lewis, W. R., Bales, K. L., Revell, D. Z., Croyle, M. J., Engle, S. E., Song, C. J., . . . Yoder, B. K. (2019). Mks6 mutations reveal tissue- and cell type-specific roles for the cilia transition zone. *FASEB J*, *33* (1), 1440-1455. doi:10.1096/fj.201801149R
- Mahjoub, M. R., Xie, Z., & Stearns, T. (2010). Cep120 is asymmetrically localized to the daughter centriole and is essential for centriole assembly. *J Cell Biol*, *191* (2), 331-346. doi:10.1083/jcb.201003009
- Mejcase, C., Hummel, A., Mohand-Said, S., Andrieu, C., El Shamieh, S., Antonio, A., . . . Audo, I. (2019). Whole exome sequencing resolves complex phenotype and identifies CC2D2A mutations underlying non-syndromic rod-cone dystrophy. *Clin Genet*, *95* (2), 329-333. doi:10.1111/cge.13453
- Mitchison, H. M., & Valente, E. M. (2017). Motile and non-motile cilia in human pathology: from function to phenotypes. *J Pathol*, *241* (2), 294-309. doi:10.1002/path.4843
- Molinari, E., Decker, E., Mabillard, H., Tellez, J., Srivastava, S., Raman, S., . . . Sayer, J. A. (2018). Human urine-derived renal epithelial cells provide insights into kidney-specific alternate splicing variants. *Eur J Hum*

Genet, 26 (12), 1791-1796. doi:10.1038/s41431-018-0212-5

Molinari, E., Ramsbottom, S. A., Srivastava, S., Booth, P., Alkanderi, S., McLafferty, S. M., . . . Sayer, J. A. (2019). Targeted exon skipping rescues ciliary protein composition defects in Joubert syndrome patient fibroblasts. *Sci Rep*, 9 (1), 10828. doi:10.1038/s41598-019-47243-z

Molinari, E., Srivastava, S., Sayer, J. A., & Ramsbottom, S. A. (2017). From disease modelling to personalised therapy in patients with CEP290 mutations. *F1000Res*, 6 , 669. doi:10.12688/f1000research.11553.1

Mougou-Zerelli, S., Thomas, S., Szenker, E., Audollent, S., Elkhartoufi, N., Babarit, C., . . . Attie-Bitach, T. (2009). CC2D2A mutations in Meckel and Joubert syndromes indicate a genotype-phenotype correlation. *Hum Mutat*, 30 (11), 1574-1582. doi:10.1002/humu.21116

Nilsen, T. W., & Graveley, B. R. (2010). Expansion of the eukaryotic proteome by alternative splicing. *Nature*, 463 (7280), 457-463. doi:10.1038/nature08909

Noor, A., Windpassinger, C., Patel, M., Stachowiak, B., Mikhailov, A., Azam, M., . . . Ayub, M. (2008). CC2D2A, encoding a coiled-coil and C2 domain protein, causes autosomal-recessive mental retardation with retinitis pigmentosa. *Am J Hum Genet*, 82 (4), 1011-1018. doi:10.1016/j.ajhg.2008.01.021

Novarino, G., Akizu, N., & Gleeson, J. G. (2011). Modeling human disease in humans: the ciliopathies. *Cell*, 147 (1), 70-79. doi:10.1016/j.cell.2011.09.014

Oberbauer, R., Schreiner, G. F., & Meyer, T. W. (1995). Renal uptake of an 18-mer phosphorothioate oligonucleotide. *Kidney Int*, 48 (4), 1226-1232. doi:10.1038/ki.1995.406

Ojeda Naharro, I., Gesemann, M., Mateos, J. M., Barmettler, G., Forbes, A., Ziegler, U., . . . Bachmann-Gagescu, R. (2017). Loss-of-function of the ciliopathy protein Cc2d2a disorganizes the vesicle fusion machinery at the periciliary membrane and indirectly affects Rab8-trafficking in zebrafish photoreceptors. *PLoS Genet*, 13 (12), e1007150. doi:10.1371/journal.pgen.1007150

Otto, E. A., Ramaswami, G., Janssen, S., Chaki, M., Allen, S. J., Zhou, W., . . . Hildebrandt, F. (2011). Mutation analysis of 18 nephronophthisis associated ciliopathy disease genes using a DNA pooling and next generation sequencing strategy. *J Med Genet*, 48 (2), 105-116. doi:10.1136/jmg.2010.082552

Pan, Q., Shai, O., Lee, L. J., Frey, B. J., & Blencowe, B. J. (2008). Deep surveying of alternative splicing complexity in the human transcriptome by high-throughput sequencing. *Nat Genet*, 40 (12), 1413-1415. doi:10.1038/ng.259

Pardridge, W. M. (2002). Drug and gene delivery to the brain: the vascular route. *Neuron*, 36 (4), 555-558. doi:10.1016/s0896-6273(02)01054-1

Parisi, M. A. (2019). The molecular genetics of Joubert syndrome and related ciliopathies: The challenges of genetic and phenotypic heterogeneity. *Transl Sci Rare Dis*, 4 (1-2), 25-49. doi:10.3233/TRD-190041

Pauli, S., Altmüller, J., Schröder, S., Ohlenbusch, A., Dreha-Kulaczewski, S., Bergmann, C., . . . Brockmann, K. (2019). Homozygosity for the c.428delG variant in KIAA0586 in a healthy individual: implications for molecular testing in patients with Joubert syndrome. *J Med Genet*, 56 (4), 261-264. doi:10.1136/jmedgenet-2018-105470

Radha Rama Devi, A., Naushad, S. M., & Lingappa, L. (2020). Clinical and Molecular Diagnosis of Joubert Syndrome and Related Disorders. *Pediatr Neurol*, 106 , 43-49. doi:10.1016/j.pediatrneurol.2020.01.012

Ramsbottom, S. A., Molinari, E., Srivastava, S., Silberman, F., Henry, C., Alkanderi, S., . . . Sayer, J. A. (2018). Targeted exon skipping of a CEP290 mutation rescues Joubert syndrome phenotypes in vitro and in a murine model. *Proc Natl Acad Sci U S A*, 115 (49), 12489-12494. doi:10.1073/pnas.1809432115

Ramsbottom, S. A., Thelwall, P. E., Wood, K. M., Clowry, G. J., Devlin, L. A., Silberman, F., . . . Miles, C. G. (2020). Mouse genetics reveals Barttin as a genetic modifier of Joubert syndrome. *Proc Natl Acad Sci*

U S A, 117 (2), 1113-1118. doi:10.1073/pnas.1912602117

Reiter, J. F., & Leroux, M. R. (2017). Genes and molecular pathways underpinning ciliopathies. *Nat Rev Mol Cell Biol*, 18 (9), 533-547. doi:10.1038/nrm.2017.60

Romani, M., Micalizzi, A., & Valente, E. M. (2013). Joubert syndrome: congenital cerebellar ataxia with the molar tooth. *Lancet Neurol*, 12 (9), 894-905. doi:10.1016/s1474-4422(13)70136-4

Roosing, S., Romani, M., Isrie, M., Rosti, R. O., Micalizzi, A., Musaev, D., . . . Valente, E. M. (2016). Mutations in CEP120 cause Joubert syndrome as well as complex ciliopathy phenotypes. *J Med Genet*, 53 (9), 608-615. doi:10.1136/jmedgenet-2016-103832

Rozet, J. M., & Gerard, X. (2015). Understanding disease pleiotropy: From puzzle to solution. *Sci Transl Med*, 7 (291), 291fs224. doi:10.1126/scitranslmed.aac6504

Schueler, M., Halbritter, J., Phelps, I. G., Braun, D. A., Otto, E. A., Porath, J. D., . . . Hildebrandt, F. (2016). Large-scale targeted sequencing comparison highlights extreme genetic heterogeneity in nephronophthisis-related ciliopathies. *J Med Genet*, 53 (3), 208-214. doi:10.1136/jmedgenet-2015-103304

Servais, L., Montus, M., Guiner, C. L., Ben Yaou, R., Annoussamy, M., Moraux, A., . . . Voit, T. (2015). Non-Ambulant Duchenne Patients Theoretically Treatable by Exon 53 Skipping have Severe Phenotype. *J Neuromuscul Dis*, 2 (3), 269-279. doi:10.3233/jnd-150100

Shaheen, R., Schmidts, M., Fageih, E., Hashem, A., Lausch, E., Holder, I., . . . Alkuraya, F. S. (2015). A founder CEP120 mutation in Jeune asphyxiating thoracic dystrophy expands the role of centriolar proteins in skeletal ciliopathies. *Hum Mol Genet*, 24 (5), 1410-1419. doi:10.1093/hmg/ddu555

Shaheen, R., Szymanska, K., Basu, B., Patel, N., Ewida, N., Fageih, E., . . . Alkuraya, F. S. (2016). Characterizing the morbid genome of ciliopathies. *Genome Biol*, 17 (1), 242. doi:10.1186/s13059-016-1099-5

Shamseldin, H. E., Shaheen, R., Ewida, N., Bubshait, D. K., Alkuraya, H., Almardawi, E., . . . Alkuraya, F. S. (2020). The morbid genome of ciliopathies: an update. *Genet Med*. doi:10.1038/s41436-020-0761-1

Srour, M., Hamdan, F. F., Schwartzentruber, J. A., Patry, L., Ospina, L. H., Shevell, M. I., . . . Michaud, J. L. (2012). Mutations in TMEM231 cause Joubert syndrome in French Canadians. *J Med Genet*, 49 (10), 636-641. doi:10.1136/jmedgenet-2012-101132

Stenson, P. D., Mort, M., Ball, E. V., Evans, K., Hayden, M., Heywood, S., . . . Cooper, D. N. (2017). The Human Gene Mutation Database: towards a comprehensive repository of inherited mutation data for medical research, genetic diagnosis and next-generation sequencing studies. *Hum Genet*, 136 (6), 665-677. doi:10.1007/s00439-017-1779-6

Szymanska, K., Berry, I., Logan, C. V., Cousins, S. R., Lindsay, H., Jafri, H., . . . Johnson, C. A. (2012). Founder mutations and genotype-phenotype correlations in Meckel-Gruber syndrome and associated ciliopathies. *Cilia*, 1 (1), 18. doi:10.1186/2046-2530-1-18

Tabrez, S. S., Sharma, R. D., Jain, V., Siddiqui, A. A., & Mukhopadhyay, A. (2017). Differential alternative splicing coupled to nonsense-mediated decay of mRNA ensures dietary restriction-induced longevity. *Nat Commun*, 8 (1), 306. doi:10.1038/s41467-017-00370-5

Tallila, J., Jakkula, E., Peltonen, L., Salonen, R., & Kestila, M. (2008). Identification of CC2D2A as a Meckel syndrome gene adds an important piece to the ciliopathy puzzle. *Am J Hum Genet*, 82 (6), 1361-1367. doi:10.1016/j.ajhg.2008.05.004

Tallila, J., Salonen, R., Kohlschmidt, N., Peltonen, L., & Kestila, M. (2009). Mutation spectrum of Meckel syndrome genes: one group of syndromes or several distinct groups? *Hum Mutat*, 30 (8), E813-830. doi:10.1002/humu.21057

- Tsai, J. J., Hsu, W. B., Liu, J. H., Chang, C. W., & Tang, T. K. (2019). CEP120 interacts with C2CD3 and Talpid3 and is required for centriole appendage assembly and ciliogenesis. *Sci Rep*, 9 (1), 6037. doi:10.1038/s41598-019-42577-0
- Uhlén, M., Fagerberg, L., Hallström, B. M., Lindskog, C., Oksvold, P., Mardinoglu, A., . . . Pontén, F. (2015). Proteomics. Tissue-based map of the human proteome. *Science*, 347 (6220), 1260419. doi:10.1126/science.1260419
- Veleri, S., Manjunath, S. H., Fariss, R. N., May-Simera, H., Brooks, M., Foskett, T. A., . . . Swaroop, A. (2014). Ciliopathy-associated gene Cc2d2a promotes assembly of subdistal appendages on the mother centriole during cilia biogenesis. *Nat Commun*, 5 , 4207. doi:10.1038/ncomms5207
- Vilboux, T., Doherty, D. A., Glass, I. A., Parisi, M. A., Phelps, I. G., Cullinane, A. R., . . . Gunay-Aygun, M. (2017). Molecular genetic findings and clinical correlations in 100 patients with Joubert syndrome and related disorders prospectively evaluated at a single center. *Genet Med*, 19 (8), 875-882. doi:10.1038/gim.2016.204
- Watson, C. M., Crinnion, L. A., Berry, I. R., Harrison, S. M., Lascelles, C., Antanaviciute, A., . . . Bonthron, D. T. (2016). Enhanced diagnostic yield in Meckel-Gruber and Joubert syndrome through exome sequencing supplemented with split-read mapping. *BMC Med Genet*, 17 , 1. doi:10.1186/s12881-015-0265-z
- Williams, C. L., Li, C., Kida, K., Inglis, P. N., Mohan, S., Semenec, L., . . . Leroux, M. R. (2011). MKS and NPHP modules cooperate to establish basal body/transition zone membrane associations and ciliary gate function during ciliogenesis. *J Cell Biol*, 192 (6), 1023-1041. doi:10.1083/jcb.201012116
- Xiao, D., Lv, C., Zhang, Z., Wu, M., Zheng, X., Yang, L., . . . Chen, J. (2017). Novel CC2D2A compound heterozygous mutations cause Joubert syndrome. *Mol Med Rep*, 15 (1), 305-308. doi:10.3892/mmr.2016.6007
- Xie, Z., Moy, L. Y., Sanada, K., Zhou, Y., Buchman, J. J., & Tsai, L. H. (2007). Cep120 and TACCs control interkinetic nuclear migration and the neural progenitor pool. *Neuron*, 56 (1), 79-93. doi:10.1016/j.neuron.2007.08.026
- Yates, A. D., Achuthan, P., Akanni, W., Allen, J., Allen, J., Alvarez-Jarreta, J., . . . Flicek, P. (2020). Ensembl 2020. *Nucleic Acids Res*, 48 (D1), D682-D688. doi:10.1093/nar/gkz966
- Yu, R. Z., Kim, T. W., Hong, A., Watanabe, T. A., Gaus, H. J., & Geary, R. S. (2007). Cross-species pharmacokinetic comparison from mouse to man of a second-generation antisense oligonucleotide, ISIS 301012, targeting human apolipoprotein B-100. *Drug Metab Dispos*, 35 (3), 460-468. doi:10.1124/dmd.106.012401
- Zhao, Q., Zhou, R., Temsamani, J., Zhang, Z., Roskey, A., & Agrawal, S. (1998). Cellular distribution of phosphorothioate oligonucleotide following intravenous administration in mice. *Antisense Nucleic Acid Drug Dev*, 8 (6), 451-458. doi:10.1089/oli.1.1998.8.451
- Zhou, X., Edmonson, M. N., Wilkinson, M. R., Patel, A., Wu, G., Liu, Y., . . . Zhang, J. (2016). Exploring genomic alteration in pediatric cancer using ProteinPaint. *Nat Genet*, 48 (1), 4-6. doi:10.1038/ng.3466

TABLES

Table 1: Patients with biallelic *CEP120* variants and associated phenotypes

Family ID	Patient ID	Phenotype	Kidney phenotype (1)	Allele 1 (Ex,Int)	Allele 2 (Ex,Int)
1	Family 1.II:2	JATD (3)	n/a	c.595G>C ; p.Ala199Pro (Ex6)	c.595G>C ; p.Ala199Pro (Ex6)
2	Family 2.II:4	JATD (3)	n/a	c.595G>C ; p.Ala199Pro (Ex6)	c.595G>C ; p.Ala199Pro (Ex6)
3	Family 3.II:1	JATD (3)	yes	c.595G>C ; p.Ala199Pro (Ex6)	c.595G>C ; p.Ala199Pro (Ex6)
4	COR391	JBTS	no	c.581T>C ; p.Val194Ala (Ex6)	c.581T>C ; p.Val194Ala (Ex6)
5	MTI-143	JBTS	no (2)	c.2177T>C ; p.Leu726Pro (Ex16)	c.2177T>C ; p.Leu726Pro (Ex16)
6	MTI-991	JBTS	no	c.49+5.49+10del ; p.Gly+1AspfsTer14 (?) (Int2)	c.49+5.49+10del ; p.Gly+1AspfsTer14 (?) (Int2)
7	MTI-1516	JBTS	no	c.1138_1139insA ; p.Ser380TyrfsTer19 (Ex9)	c.1138_1139insA ; p.Ser380TyrfsTer19 (Ex9)

Family ID	Patient ID	Phenotype	Kidney phenotype (1)	Allele 1 (Ex,Int)	Allele 2 (Ex,Int)
8	MKS-2930	MKS/OFD	yes	c.2924T>G ; p.Ile975Ser (Ex21)	c.2924T>G ; p.Ile975Ser (Ex21)
9	SW-476410	TCDOE	no	c.451C>T ; p.Arg151Ter (Ex5)	c.595C>T ; p.Arg151Ter (Ex5)

CEP120 transcript: NM.153223.3.

JATD, Jeune asphyxiating thoracic dystrophy; JBTS, Joubert syndrome; MKS, Meckel syndrome; OFD, oro-facial-digital syndrome; TCDOE, tectocerebellar dysraphia with occipital encephalocele.

(1) Designated as n/a, unless renal phenotype clearly stated.

(2) For this patient Roosing et al., (Roosing et al., 2016) reported: grade II-III hydronephrosis was detected at birth but it spontaneously resolved after few months. No renal problems have been reported since then.

(3) A fourth JATD case was described (Shaheen et al., 2015), however DNA from the proband was not available. Both parents presented the *CEP120* : p.Ala199Pro variant in heterozygosis.

Table 2: Patients with truncating *CC2D2A* variants in potentially skippable exons and associated phenotypes

Family ID (9)	Patient ID	Phenotype	Kidney phenotype (2)	Allele 1 (Ex,Int)
15	UW41-IV:1	JSRD	no	c.2848C>T ; p.Arg950Ter (Ex23)
16	UW47-II:1	JBTS	no	c.3055C>T ; p.Arg1019Ter (Ex25)
20	UM10	MKS	n/a	c.3084del ; p.Lys1029ArgfsTer3 (Ex25)
26	MKS-54	MKS	yes	c.517C>T ; p.Arg173Ter (Ex8)
29	MKS-977	MKS	yes	c.3084del ; p.Lys1029ArgfsTer3 (Ex25)
33	MKS-365	MKS	yes	c.2773C>T ; p.Arg925Ter (Ex22) (?) (3)
34	UW67	JSRD	yes	c.3347C>T ; p.Thr1116Met (Ex27)
35	F434-21	JSRD	no	c.517C>T ; p.Arg173Ter (Ex8)
36	A2421-21	MKS	yes	c.3544T>C ; p.Trp1182Arg (Ex29)
38	M506	MKS	n/a	c.3084del ; p.Lys1029ArgfsTer3 (Ex25)
40	UW75-3	JBTS	no	c.1676T>C ; p.Leu559Pro (Ex16)
42	UW78-3	JBTS	n/a	c.3055C>T ; p.Arg1019Ter (Ex25)
43	UW79-3	JBTS	no	c.1263_1264insGGCATGTTTTGGC ; p.Ser422Gly (Ex25)
43	UW79-4	JBTS	no	c.1263_1264insGGCATGTTTTGGC ; p.Ser422Gly (Ex25)
51	128	MKS	n/a	c.3544T>C ; p.Trp1182Arg (Ex29)
61		MKS	yes	c.3774dup ; p.Glu1259Ter (Ex31)
62	MTI-127	JBTS/JSRD (5)	n/a	c.4583G>A ; p.Arg1528His (Ex37) (6)
67	3	JBTS/MKS (8)	n/a	c.2803C>T ; p.Arg935Ter (Ex22)
68	4	JBTS/MKS (8)	n/a	c.2875del ; p.Glu959AsnfsTer3 (Ex23)
69	FT-1	MKS	yes	c.3084del ; p.Lys1029ArgfsTer3 (Ex25)
73	FT-15	MKS	yes	c.3084del ; p.Lys1029ArgfsTer3 (Ex25)
74	FT-21	MKS	yes	c.3084del ; p.Lys1029ArgfsTer3 (Ex25)
76	F850-21	Cogan	yes	c.1267C>T ; p.Arg423Ter (Ex13)
79		JSRD	yes	c.2581G>A ; p.Asp861Asn (Ex21)
84	44:36	JBTS	no	c.3744_3747dup ; p.Pro1250GlyfsTer11 (Ex30) (9)
84	45:36	JBTS	no	c.3744_3747dup ; p.Pro1250GlyfsTer11 (Ex30) (9)

CC2D2A transcript: NM.001080522.2.

Cogan, Cogan-type congenital oculomotor apraxia; JBTS, Joubert syndrome; JSRD, Joubert syndrome related disorders; MKS, Meckel syndrome; ML, Meckel-like syndrome.

- (1) Relates to family ID of complete database in Table S3.
- (2) Designated as n/a, unless renal phenotype clearly stated.
- (3) Variant initially reported as c.2673C>T ; p.Arg925Ter.
- (4) Variant initially reported as c.1263_4InsGGCATGTTTTTGGC; c.1268G>A ; p.(Ser423Glyfs*19).
- (5) Study does not precise phenotype.
- (6) Variant initially reported as c.4258G>A ; p.(Arg1528His). This variant was found corrected as c.4583G>A ; p.(Arg1528His) (Lam et al., 2020).
- (7) Variant initially reported as c.1412delG ; p.(Lys472Argfs*). This variant was found corrected as c.3082del ; p.(Arg1028Glyfs*4)f (Ben-Salem, Al-Shamsi, Gleeson, Ali, & Al-Gazali, 2015).
- (8) In this study (Watson et al., 2016), patients were referred with a clinical diagnosis of either JBTS (9 patients) or MKS (17 patients). The genetic diagnosis was confirmed in 14 of the 26 cases, a diagnostic yield of 54%. The exact phenotype is not reported.
- (9) Variant initially reported as c.3743_3746dup; p.(Pro1250Glyfs*11).

FIGURE LEGENDS

Figure 1. Phenotypes and genotypes in patients carrying biallelic *CC2D2A* variants

A. Distribution of phenotypes associated with *CC2D2A* biallelic variants in reported patients. n indicates total number of patients. ASD, autism spectrum disorder; Cogan, Cogan-type congenital oculomotor apraxia; JBTS, Joubert syndrome; JSRD, Joubert syndrome related disorders; MKS, Meckel syndrome; ML, Meckel-like syndrome; RCD, rod cone dystrophy; ?, not unequivocally described. B. Distribution of *CC2D2A* variant consequences detected in index patients. n indicates total number of alleles. AAdel, single amino acid deletion; Large ins/del, large insertions/deletion including retrotransposon insertion. C. Distribution of *CC2D2A* allelic status detected in patients with Meckel syndrome or Meckel-like syndrome. D. Distribution of *CC2D2A* allelic status detected in patients with Joubert syndrome or Joubert syndrome related disorders. E. Distribution of *CC2D2A* allelic status detected in patients with kidney disease. F. Distribution of *CC2D2A* allelic status detected in patients without kidney disease. Truncating indicates either a nonsense or a frameshift variant.

Figure 2. Exon usage and tissue specific transcript expression of *CEP120* and *CC2D2A*

Ai. *CEP120* predicted protein coding transcript isoforms with highest expression levels in kidney medulla (red) and cerebellar hemisphere (blue) based on RNA sequencing data from the Genotype-Tissue Expression (GTEx) Project. Aii. *CEP120* genomic localization, the different exons detected in GTEx data with the different imputed splice junctions and the three transcripts detected at highest levels in kidney medulla and cerebellar hemisphere. Exons are labelled with respect to transcript ENST00000328236. The open reading frame is shown in dark grey with the start codon marked with an arrowhead. Aiii. Predicted protein products from the three analyzed transcripts. Bi. *CC2D2A* predicted protein coding transcript isoforms with highest expression levels in kidney medulla (red) and cerebellar hemisphere (blue) based on RNA sequencing data from the Genotype-Tissue Expression (GTEx) Project. Bii. *CC2D2A* genomic localization, the different exons detected in GTEx data with the different imputed splice junctions and the three transcripts detected at highest levels in kidney medulla and cerebellar hemisphere. Exons are labelled with respect to transcript ENST00000503292. The open reading frame is shown in dark grey with the start codon marked with an arrowhead. Junction reads enriched in the kidney medulla (compared to cerebellum) or marked in red and junction reads enriched in the cerebellum (compared to kidney) are marked in blue. Biii. Predicted protein products from the three analyzed transcripts, sequences deviating from reference sequence are depicted in orange. The Genotype-Tissue Expression (GTEx) Project was supported by the Common Fund of the Office of the Director of the National Institutes of Health, and by NCI, NHGRI, NHLBI, NIDA, NIMH, and

NINDS. The data used for the analyses described in this manuscript were obtained from the GTEx Portal on 15/05/2020.

Figure 3. Basal exon skipping of *CC2D2A* exon 30 in kidney and human urine-derived renal epithelial cells (hURECs) and correlation with tissue specific disease expression

A. RT-PCR using RNA isolated from human kidney, whole blood and hURECs. *CC2D2A* primer pair (arrows) designed to detect exon 30 skipping illustrated on the right. Note shortened transcript at ~150bp (*asterisk) detected in kidney and hURECs suggesting basal exon 30 skipping. B. Prevalence of kidney disease associated with truncating *CC2D2A* variants in different exons. Exons are labelled according to transcript ENST00000328236. The different exons and possible splice junctions detected in GTEx are shown below transcript ENST00000328236. The specific splice junction leading to basal exon 30 skipping in the kidney is marked in diagonal shading. N indicates the total number of patients (with and without kidney disease) harboring at least one truncating variants in the corresponding exons. 35/48 (73%) present with kidney disease. Note that both patients with a truncating variant in exon 30, undergoing basal exon skipping in the kidney, have no reported kidney disease (0%).

Figure 4: Distribution of mutations in *CEP120* and *CC2D2A* and identification of potential targets for exon skipping

A. *CEP120* mRNA (NM_153223.3) and exon structure with UTR in grey. Exon numbers are shown below exons with nucleotide numbers in multiples of three below the exon numbers. Exact multiples of three are shown in green. Protein domains are shown in color-code for coiled-coil domain (CC) and the 3 C2 domains. Detected *CEP120* variants are painted above the mRNA structure with respect to their location and allelic frequency in index patients. Variant consequences are color-coded as indicated. Exon numbers that appear as candidates for exons skipping based on nucleotide numbers and domain functions are shaded in green, while candidates arising from tissue-specific transcript analysis are shaded in blue. B. *CC2D2A* mRNA (NM_001080522.2) and exon structure with UTR in grey. Exon numbers are shown below exons with nucleotide numbers in multiples of three below the exon numbers. Exact multiples of three are shown in green. Protein domains are shown in color-code for coiled-coil domain 1 and 2 (CC) and the C2 domain. Exon numbers that appear as candidates for exons skipping based on nucleotide numbers and domain functions are shaded in green, candidates arising from tissue-specific transcript analysis are shaded in blue and possible candidate based on conflicting domain annotation shaded in turquoise. Only truncating *CC2D2A* variants that are reported in candidate exons for exon skipping are painted above the mRNA structure with respect to their location and allelic frequency in index patients. Variant consequences are color-coded as indicated. The retrotransposon insertion described in one family is not represented.

Figure 1

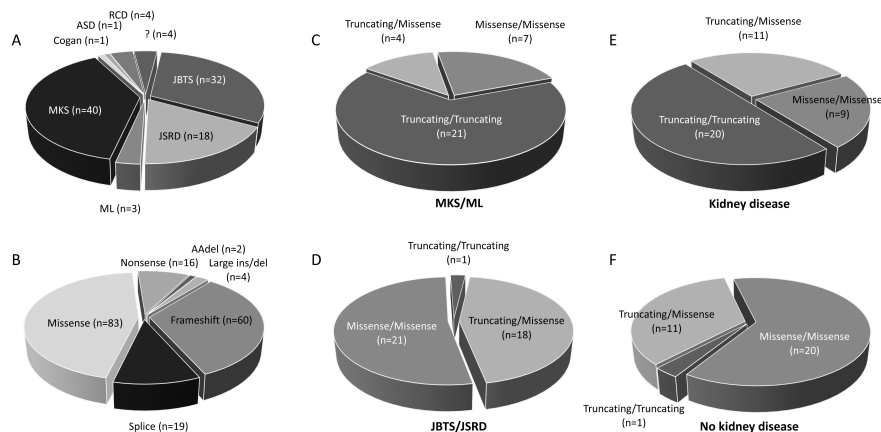


Figure 2

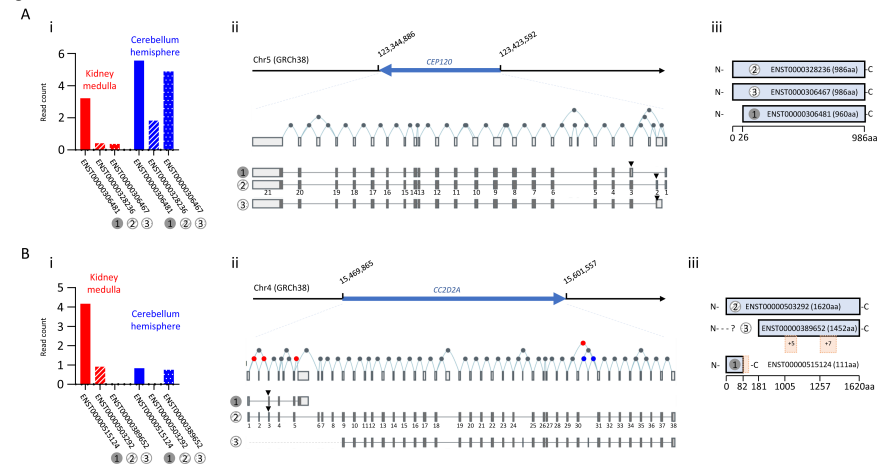


Figure 3

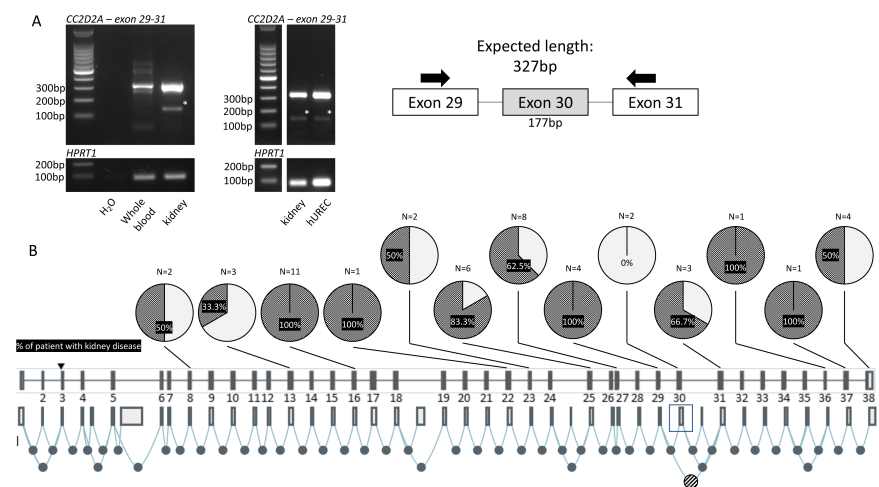


Figure 4

